Interaction Energies for Blends of Poly(methyl methacrylate), Polystyrene, and Poly(α-methylstyrene) by the Critical Molecular Weight Method

T. A. Callaghan† and D. R. Paul*

Department of Chemical Engineering and Center for Polymer Research, The University of Texas at Austin, Austin, Texas 78712

Received November 13, 1992; Revised Manuscript Received January 29, 1993

ABSTRACT: Interaction energies for each of the binary pairs PS/Pα-MS, PS/PMMA, and PMMA/Pα-MS were calculated by fitting spinodal curves predicted by the Flory–Huggins theory and the Sanchez–Lacombe equation of state theory to experimental cloud point data for blends of low molecular weight polymers. For blends of PS and Pα-MS, where cloud points could not be observed, the molecular weight limit of miscibility was used to bracket the interaction energy. Phase separation boundaries for this system were predicted to be caused by UCST-type behavior. Oligomeric blends of PMMA with PS showed UCST-type phase boundaries while blends of PMMA with Pα-MS showed LCST-type boundaries. The mechanism of phase separation boundaries was found to stem from the differences between the characteristic temperatures for the pure components (ΔT^*). End groups on the oligomeric homopolymers significantly affect the calculated interaction energies, and corrections for this were made by three methods including a binary interaction model analysis.

Introduction

There is a strong interest in polymer blends as a route to new products which may show a continuous range of properties.[1–6] However, whether blends yield additive or useful properties or not often hinges on the thermodynamic interaction between the component polymers. If this is favorable enough to achieve miscibility, then additivity of properties is essentially assured. However, useful materials may be achieved by optimizing this interaction to something just short of miscibility. In any case there is an important fundamental need to know more about polymer/polymer interactions and how to design polymers for desired levels of interactions (including miscibility) with other polymers.

This paper is the first in a series aimed at quantitatively establishing interaction energies between polycarbonates or polysulfones with polymers composed of common double-bonded monomers like styrene (S), α-methylstyrene (α-MS), or methyl methacrylate (MMA) which are relatively inexpensive and widely used. Blends of such polymers with more expensive engineering thermoplastics (i.e., polycarbonates and polysulfones) are of great commercial interest. Many methods are used for determining the interaction parameters such as melting point depression,[7,8] heat of dilution,[9] analog calorimetry,[10] neutron scattering,[11] or sorption probe techniques.[12,13] Each technique has its own merits and limitations and there is no one method suitable for all situations.

A recent technique described by Kambour et al.[14] involves finding the critical molecular weights at which a polymer pair becomes miscible. As the molecular weight is decreased the combinatorial entropy of mixing becomes more favorable and eventually may overcome an unfavorable enthalpy of mixing and cause the blend to be miscible. Obviously, this approach is limited to pairs with positive interaction energies (endothermic mixing), but this will encompass the types of interactions of interest here. If the only observation from the available discrete steps in molecular weight is a change from immiscible to miscible, then this technique can only bracket the interaction energy. However, if it is possible to observe phase separation boundaries either on heating or on cooling, the interaction energy can be quantitatively evaluated. Most low molecular weight polymers show UCST-type phase boundaries, but LCST-type phase boundaries occur if the component polymers have large differences in thermal expansion coefficients.[15] Miscible blends of high molecular weight polymers commonly show LCST behavior.

Both the Flory–Huggins theory and the Sanchez–Lacombe equation of state theory,[16–19] combined with the binary interaction model when appropriate,[20–22] will be used here to analyze the experimentally observed phase behavior. The equation of state theory allows for the compressible nature of the polymers and permits prediction of lower critical solution temperature behavior, which is not possible with the classical Flory–Huggins theory without assigning a temperature dependence to the interaction energy. Both theories will be used to quantify interaction energies which will allow us to assess the effects of compressibility.

Interaction energies for the polymer pairs studied here have been reported previously, so some comparisons with other techniques are possible. We specifically deal with the issue of temperature dependence of the interaction energies and with end group effects that can be a significant factor in the phase behavior of oligomer blends. The results presented here represent an important step in building an interaction energy database that will be used in future studies concerning blends with polycarbonates and polysulfones.

As shown here, when the molecular weight becomes low enough it may be necessary to account for any end groups that are different from the repeat unit. The end groups can affect the temperature at which phase separation occurs on heating (LCST) or cooling (UCST). Both LCST-type phase behavior and UCST-type phase behavior are observed in the following.

Materials and Procedures

The polymers used are described in Table I. All homopolymers were supplied by Polymer Laboratories Ltd. and are essentially monodisperse except for the commercial polystyrene, Cosden 550, supplied by Cosden Oil and Chemical Co., who specified its molecular weight as $\bar{M}_w$ = 330 000 and $\bar{M}_n$ = 100 000. The value given here ($\bar{M}_w$ = 341 000) was determined by light scattering

* To whom all correspondence should be addressed.
† Current address: Dow Chemical Co., Plaquemine, LA 70765.

0024-9297/93/2226-2439$04.00/0

Table I. Polymers Used in This Work

polymer	designation[a]	$\bar{M}_w$[b]	$\bar{M}_w/\bar{M}_n$[b]	T_g (°C)	density (g/cm^3) at 30 °C	end group (wt %)
poly(methyl methacrylate)	PMMA(1.21)	1210	1.16	31	1.173	11.5
poly(methyl methacrylate)	PMMA(2.4)	2400	1.09	77	1.184	5.41
poly(methyl methacrylate)	PMMA(4.25)	4250	1.07	99	1.188	3.00
poly(methyl methacrylate)	PMMA(10.55)	10550	1.11	108	1.191	1.25
poly(methyl methacrylate)	PMMA(20.3)	20300	1.11	125	1.192	0.652
polystyrene	PS(.580)	580	1.18	−23	0.9960	11.5
polystyrene	PS(.680)	680	1.16	−6	1.0087	9.76
polystyrene	PS(0.950)	950	1.13	6	1.0260	6.81
polystyrene	PS(2.95)	2950	1.05	74	1.039	2.03
polystyrene	PS(9.2)	9200	1.03	96	1.045	0.640
polystyrene	PS(22)	22000	1.03	102	1.046	0.267
polystyrene	PS(52)	52000	1.03	106	1.047	0.113
polystyrene	PS(341)	341000[c]	3.3	105	1.048	
poly(α-methylstyrene)	Pα-MS(3.5)	3500	1.06	141	1.054	1.73
poly(α-methylstyrene)	Pα-MS(6.7)	6700	1.06	160	1.058	0.90
poly(α-methylstyrene)	Pα-MS(19.5)	19500	1.03	169	1.061	0.30
poly(α-methylstyrene)	Pα-MS(55)	55000	1.03	180	1.062	0.14

[a] The number in parentheses corresponds to the weight-average molecular weight in thousands. [b] Molecular weight information from supplier (Polymer Laboratories Ltd.). [c] Determined from light scattering in this laboratory.

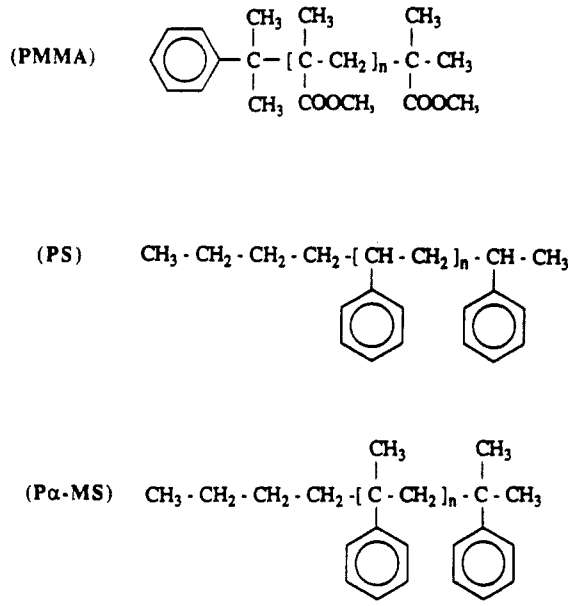

Figure 1. Polymer repeat units with end groups as given by supplier.[24]

in this laboratory. Molecular weights listed for the polymers supplied by Polymer Laboratories Ltd. are the peak molecular weight from GPC, which essentially corresponds to $\bar{M}_w$ according to company literature.[23]

The monodisperse polymers were synthesized via anionic polymerization using an organometallic species for initiation. The initiating species results in end groups which are dissimilar from the repeat unit. These end groups can affect the interaction energies for oligomer mixtures; this effect diminishes as the molecular weight of the polymer increases and becomes negligible at high molecular weights. The end group types on each polymer, as identified by the supplier,[24] are shown in Figure 1 and their concentrations are included in Table I. The organometallic initiator used for both PS and Pα-MS synthesis was *n*-butyllithium, while the initiator for PMMA is believed to be cumylcesium, which can be prepared by Ziegler's method[25] from methyl cumyl ether and cesium metal.[26]

Densities for solid samples were determined by a density gradient column (Techne, DC-1), based on calcium nitrate solutions, while those for liquid samples were measured by a densimeter (Antonn Parr, DMA 602) both of which were operated at 30 °C. Glass transition temperatures were determined using a Perkin-Elmer DSC-7 system with a heating rate of 20 °C/min. Glass transition temperatures were taken as the midpoint of the transition in heat capacity.

Blends were cast onto glass plates heated to ~50 °C from a 2% polymer solution in methylene chloride or tetrahydrofuran (THF). Blends were subsequently dried in a vacuum oven for 5 days at 120 °C.

Cloud points were determined optically on a hot stage (Mettler, FP 82 HT) equipped with a temperature controller (Mettler, FP 80 HT). Blends cast on glass slides were used for this purpose. The cloud point was taken as the temperature at which the blend first becomes cloudy. For blends with UCST behavior, the sample was first heated above the UCST until clear. The temperature was then lowered and the sample annealed at the desired temperature; this was repeated at lower temperatures until the blend became cloudy. Cloud points for blends with LCST behavior were determined in an analogous fashion except the temperature was raised and the sample annealed until the blend became cloudy. Cloud points for these low-$\bar{M}_w$ polymers are reversible. Three determinations for each sample were taken using at least two samples for each blend and averaged. Typically, the variation among individual determinations was no more than ±3 °C.

Changes in specific volume as a function of temperature and pressure were measured using a Gnomix *PVT* apparatus described elsewhere.[27] Samples are compressed along various isotherms, from 30 to 280 °C, with volume data recorded at pressures from 10 to 200 MPa at 24 different pressures. The volume at zero pressure for each isotherm is obtained by extrapolation of the data fitted to the Tait equation.[28-30] Data in the liquid state were fitted to the Sanchez–Lacombe equation of state to determine the characteristic parameters.[16-19,31-34] A nonlinear least squares fit was performed minimizing the quantity

$$S^2 = \sum_i \frac{(P_{i,\text{data}} - P_{i,\text{fit}})^2}{N-3} \tag{1}$$

where N is the number of data points, P_{data} is the experimental pressure at a given value of (V,T), and P_{fit} is the value of the pressure predicted by the equation of state.[35]

Background and Theory

The change in the Gibbs free energy per unit volume, Δg, can be expressed as a sum of combinatorial entropy[36,37] and noncombinatorial terms according to the classical Flory–Huggins theory as follows:

$$\Delta g_{\text{mix}} = RT\left[\sum_{i=1}^{2} \frac{\phi_i \ln \phi_i}{\tilde{V}_i}\right] + B\phi_1\phi_2 \tag{2}$$

where R is the universal gas constant, T is the absolute temperature, and ϕ_i and $\tilde{V}_i$ are the volume fraction and molar volume of component i, respectively. The noncombinatorial term in this theory employs the van Laar form[38] where B is the Flory–Huggins interaction energy density. The change in Gibbs free energy must be negative

to attain miscibility but to ensure stability its curvature must be positive. Differentiation of eq 2 gives the spinodal condition

$$\frac{d^2\Delta g}{d\phi_1^2} = RT\left[\frac{1}{\phi_1\bar{V}_1} + \frac{1}{\phi_2\bar{V}_2}\right] - 2B_{sc} = 0 \qquad (3)$$

where B_{sc} is the interaction parameter at the spinodal condition, which is equal to B in eq 2 if B is independent of composition and temperature as pointed out by Sanchez.[34] Otherwise, the two are related by the following differential equation:

$$B_{sc} = B(T) + (\phi_1 - \phi_2)\frac{dB(T)}{d\phi_1} - \frac{1}{2}\phi_1\phi_2\frac{d^2B(T)}{d\phi_1^2} \qquad (4)$$

Solving for B_{sc} in eq 3 gives

$$B_{sc} = \frac{RT}{2}\left(\frac{1}{\phi_1\bar{V}_1} + \frac{1}{\phi_2\bar{V}_2}\right) \qquad (5)$$

which defines the spinodal curve. At this point the subscript sc on B will be dropped and B will be understood to mean B_{sc} unless otherwise stated. At the critical temperature, T_c, and composition, ϕ_{1c},

$$\phi_{1c} = \frac{1}{1 + (\bar{V}_1/\bar{V}_2)^{1/2}} \qquad (6)$$

eq 5 reduces to

$$B_c = \frac{RT_c}{2}\left(\frac{1}{\bar{V}_1^{1/2}} + \frac{1}{\bar{V}_2^{1/2}}\right)^2 \qquad (7)$$

The molar volume is equal to the molecular weight divided by density, and accurate values for both are required, especially when $\bar{V}_1 \neq \bar{V}_2$. For polydisperse polymers Koningsveld and co-workers[39-42] have shown that the thermodynamic equations are similar and that the weight-average molecular weight should be used to determine the molar volume. The location of the critical point becomes

$$\phi_{1c} = \frac{1}{1 + (a_2\rho_2\bar{M}_{w,1}/a_1\rho_1\bar{M}_{w,2})^{1/2}} \qquad (8)$$

where $a_1 = \bar{M}_{z,1}/\bar{M}_{w,1}$. Generally, the critical point slides along the binodal curve on the branch for the polymer with the larger polydispersity. The spinodal curve will additionally be skewed in the direction of the polymer with the lower molecular weight.

If B is assumed to be independent of temperature, the Flory–Huggins theory will only predict UCST-type phase boundaries. This can be circumvented by allowing B to be temperature dependent, [$B(T) = B^h - TB^s$], and basic thermodynamic relations reveal that the interaction parameter is now not strictly an ethalpic parameter but also has an excess noncombinatorial entropic contribution $-T\Delta S^e_x = -TB^s\phi_1\phi_2$. This extended Flory–Huggins theory is in principle able to describe LCST-type phase separation.

While the extended Flory–Huggins theory can predict LCST-type phase separation, the compressibility of the mixture is not taken into account. There are numerous equations of state[43-47] which can account for the finite compressibility of mixtures without resorting to the empiricism used in the extended Flory–Huggins theory. It is enticing to force these equations of state into a form similar to the extended Flory–Huggins theory. This method groups the temperature and composition dependencies of the Flory–Huggins interaction parameter and explains them in terms of equation of state effects. The following discussion will be limited to the Sanchez–Lacombe equation of state theory,[16-19,31-34] which is described briefly below.

The configurational Gibbs free energy per hard core volume of mixture, $G/(rNv^*)$, presented by Sanchez can be written

$$g = \frac{G}{rNv^*} = \left[\frac{kT}{v^*}\sum_i\frac{\phi_i}{r_i}\ln\phi_i\right] - \tilde{\rho}P^* + P\tilde{v} + \frac{kT}{v^*}\left[\frac{1-\tilde{\rho}}{\tilde{\rho}}\ln(1-\tilde{\rho}) + \frac{1}{r}\ln\tilde{\rho}\right] \qquad (9)$$

Here, N is the number of polymer chains, v^* is the hard core volume of a mer, and r is the chain length defined as

$$r = \frac{MP^*}{kT^*\rho^*} = \frac{M}{v^*\rho^*} \qquad (10)$$

where M is the weight-average molecular weight. Reduced variables are given by

$$\tilde{P} = P/P^*; \quad \tilde{T} = T/T^*; \quad \tilde{\rho} = \rho/\rho^* = 1/\tilde{v} \qquad (11)$$

At equilibrium the free energy is at a minimum and the equation of state is

$$\tilde{\rho}^2 + \tilde{P} + \tilde{T}\left[\ln(1-\tilde{\rho}) + \left(1 - \frac{1}{r}\right)\tilde{\rho}\right] = 0 \qquad (12)$$

For polymer liquids where $r \to \infty$, the equation of state reduces to a simple corresponding states equation. Mixing rules are required in all statistical mechanical theories and are often quite arbitrary; the ones used here are those outlined by Sanchez.[19] Each pure component has its own mer volume v^*_i, but in the mixture all mers are required to have the same average volume v^*. Thus, a molecule i will occupy r°_i sites and have a volume of $r^\circ_i v^*_i$ in the pure close-packed state. In the mixture it will occupy r_i sites such that $r^\circ_i v^*_i = r_i v^*$. The rest of the mixing rules follow and are given by

$$\frac{1}{v^*} = \sum_i\frac{\phi_i}{v^*_i}; \quad \frac{1}{\rho^*} = \sum_i\frac{w_i}{\rho^*_i}; \quad \frac{1}{r^*} = \sum_i\frac{\phi_i}{r_i} \qquad (13)$$

where ϕ_i is the hard core volume fraction and w_i is the weight fraction. The characteristic pressures for the mixture are pairwise additive and given as

$$P^* = \sum_i\phi_i P^*_i - \sum_{i<j}\sum\phi_i\phi_j\Delta P^* \qquad (14)$$

where ΔP^* is the characteristic energy density of the blend between components i and j. This has also been called the "bare" interaction parameter[34] because of its relation to B. The interaction parameter B, inherently, includes all the equation of state effects, whereas ΔP^* is the actual energetic interaction between components after equation of state effects have been stripped away.

Both ΔH and ΔS can be derived from the lattice–fluid theory along with the mixing rules, eq 13, as shown elsewhere.[48] The interaction parameters of the extended Flory–Huggins theory can be written in terms of the Sanchez–Lacombe theory, assuming that the volume fractions in both theories are essentially equal.[48] The interaction energy associated with the heat of mixing is given by

$$B^h = \tilde{\rho}\Delta P^* + \left[\frac{P^*_1}{\phi_2}(\tilde{\rho}_1 - \tilde{\rho}) + \frac{P^*_2}{\phi_1}(\tilde{\rho}_2 - \tilde{\rho})\right] + \frac{P}{\phi_1\phi_2}(\tilde{v} - \phi_1\tilde{v}_1 - \phi_2\tilde{v}_2) \qquad (15)$$

and similarly the excess entropy term is

$$-TB^s = -\frac{kT}{\phi_1\phi_2 v^*}\left[\left(\frac{1-\tilde{\rho}}{\tilde{\rho}}\right)\ln(1-\tilde{\rho}) + \frac{\ln\tilde{\rho}}{r}\right] + \frac{kT}{(\phi_1+\nu\phi_2)v^*}\left[\frac{\tilde{v}_1}{\phi_2}\left\{(1-\tilde{\rho}_1)\ln(1-\tilde{\rho}_1) + \frac{\tilde{\rho}_1}{r^\circ_1}\ln\tilde{\rho}_1\right\} + \frac{\nu\tilde{v}_2}{\phi_1}\left\{(1-\tilde{\rho}_2)\ln(1-\tilde{\rho}_2) + \frac{\tilde{\rho}_2}{r^\circ_2}\ln\tilde{\rho}_2\right\}\right] \quad (16)$$

where ν is the ratio v^*_1/v^*_2. The mixture will be stable if the derivative of the chemical potential with respect to composition is positive over the entire composition range, i.e.

$$\frac{d\mu_1}{d\phi_1} = r_1\phi_2\left\{\frac{kT}{2v^*}\left[\frac{1}{r_1\phi_1} + \frac{1}{r_2\phi_2}\right] - \tilde{\rho}\left[\Delta P^* + \frac{kT}{2v^*}(\Psi^2\tilde{T}P^*\beta)\right]\right\} > 0 \quad (17)$$

where β is the isothermal compressibility of the mixture and

$$\Psi = \left\{\tilde{\rho}\left[\nu\left(\frac{1}{\tilde{T}_1} - \frac{1}{\tilde{T}_2}\right) + \frac{(\phi_1^2 - \nu\phi_2^2)\Delta P^* v_1}{kT}\right] - \nu\left(\frac{1}{r^\circ_1} - \frac{1}{r^\circ_2}\right) + \frac{\tilde{P}\tilde{v}}{\tilde{T}}(\nu-1)(\phi_1+\nu\phi_2)\right\}/(\phi_1+\nu\phi_2)^2 \quad (18)$$

$$\tilde{T}P^*\beta = \frac{\tilde{v}}{\frac{1}{\tilde{v}-1} + \frac{1}{r} - \frac{2}{\tilde{v}\tilde{T}}} \quad (19)$$

The term $\Psi^2\tilde{T}P^*\beta$ tends to destabilize the mixture and grows in magnitude as the temperature is raised. At some temperature this term may become greater in magnitude than the sum of the other terms in eq 17; hence, the blend will phase separate via an LCST. The Flory–Huggins equation for the spinodal condition, eq 5, can be recast in terms of the Sanchez–Lacombe theory to give

$$B_{sc} = \tilde{\rho}\Delta P^* + \left\{[P^*_2 - P^*_1 + (\phi_2-\phi_1)\Delta P^*] + \frac{RT}{\tilde{\rho}}\left(\frac{1}{r^\circ_1 v^*_1} - \frac{1}{r^\circ_2 v^*_2}\right) - RT\left[\frac{\ln(1-\tilde{\rho})}{\tilde{\rho}^2} + \frac{1}{\tilde{\rho}}\right]\left[\frac{1}{v^*_1} - \frac{1}{v^*_2}\right]\right\}^2 \Big/ \left\{\frac{2RT}{v^*}\left[\frac{2\ln(1-\tilde{\rho})}{\tilde{\rho}^3} + \frac{1}{\tilde{\rho}^2(1-\tilde{\rho})} + \frac{1-1/r}{\tilde{\rho}^2}\right]\right\} \quad (20)$$

It can be seen that B_{sc} is composed of a purely energetic term and an additional term containing both energetic and entropic contributions due to the compressibility of the mixture.

The literature[20-22] reveals that copolymerization can be used to manipulate the interaction energies and to achieve miscibility. A simple binary interaction model[20-22] leads to an expression in terms of monomer unit pair interactions, B_{ij}, for the Flory–Huggins interaction energy density for mixing a random copolymer composed of units 1 and 2 with a homopolymer of 3 units

$$B = B_{13}\phi_1' + B_{23}\phi_2' - B_{12}\phi_1'\phi_2' \quad (21)$$

where ϕ_i' indicate the volume fraction of component i in the copolymer. For the more general case of mixing two random copolymers 1,2 and 3,4, the following applies:

$$B = B_{13}\phi_1'\phi_3'' + B_{23}\phi_2'\phi_3'' + B_{14}\phi_1'\phi_4'' + B_{24}\phi_2'\phi_4'' - B_{12}\phi_1'\phi_2' - B_{34}\phi_3''\phi_4'' \quad (22)$$

where the double primes denote the 3,4 copolymer composition. By analogy to eq 21, the net interaction energy in the Sanchez–Lacombe theory[49] can be written

$$\Delta P^* = \Delta P^*_{13}\phi_1' + \Delta P^*_{23}\phi_2' - \Delta P^*_{12}\phi_1'\phi_2' \quad (23)$$

where the volume fractions can be calculated from the hard core volumes.

Table II. Summary of Blend Results

blend[a]	no. of T_g's	film appearance	exptl phase boundary	comments[b]
PS/Pα-MS				
22/55	1	clear		
52/55	1	clear		
341/55	2	clear		1
PS/PMMA				
2.95/2.4	1	clear		2
1.95/4.25	2	cloudy/clear	UCST	3, 4
2.95/10.55	2	cloudy/clear	UCST	3, 4
2.95/20.3	2	cloudy/clear	UCST > 250 °C	4, 5
2.95/60	2	cloudy/clear	UCST > 300 °C	4, 5
9.2/2.4	2/1	cloudy/clear	UCST	4, 6
9.2/4.25	1	cloudy/clear	UCST	2, 4
PMMA/Pα-MS				
1.21/6.7	1	clear		
1.21/19.5	1	clear		
2.4/3.5	1	clear		
2.4/6.7	1/2	clear/cloudy	LCST	4, 7
4.25/3.5	1/2	clear/cloudy	LCST	4, 7
4.25/6.7	1/2	clear/cloudy	LCST	4, 7
10.55/3.5	1/2	clear/cloudy		8, 9
10.55/6.7	2	cloudy		

[a] Number indicates $\bar{M}_w$ in thousands. [b] Comments: (1) Refractive indices are similar; (2) pure component T_g's are too close to resolve by DSC; (3) blends could not be trapped in homogeneous state by quenching; (4) blends were clear or cloudy depending upon the temperature; (5) UCST-type phase boundaries are at temperatures too high to be reliable; (6) blends could be trapped in homogeneous state by quenching; (7) blends could be trapped in heterogeneous state by quenching; (8) blends displayed LCST-type characteristics but nor reversible; (9) blends were clear on first heat but cloudy after heating above the T_g.

Results and Discussion

PS and Pα-MS Blends. Blends of PS and Pα-MS have been investigated extensively.[50-60] Flory–Huggins interaction energy density values reported for this pair range from 0.011 to 0.050 cal/cm^3. It has been reported that blends of low molecular weight components are miscible while immiscibility occurs when both molecular weights are above 70 000.[54] In this work miscible blends were found when the component molecular weights were as great as 52 000 for PS and 55 000 for Pα-MS. When the molecular weight of PS was raised to 341 000 (commercial grade), blends became immiscible. The PS/Pα-MS blends investigated are summarized in Table II. The single T_g found for the miscible blends was well represented by the Fox equation.

None of the blends showed phase separation boundaries on heating or cooling. The interaction energy is calculated to lie within the range $0.012 < B < 0.025$ cal/cm^3. These limits were calculated using eq 7 with values of molecular weights for the pair that was miscible to give the upper limit and the pair that was immiscible for the lower limit with T_c set equal to 50 °C, the casting temperature.

To gain insight about the mechanism by which the blend changes from miscible to immiscible (i.e., whether the

Table III. Specific Volume (cm³/g) of Pα-MS(55) as a Function of Temperature and Pressure in the Liquid State

P (MPa)	T (°C) 189.9	200.1	208.8	219.4	229.6	239.8	250.2	261.1
0	0.9781	0.9829	0.9879	0.9961	1.0003	1.0047	1.0121	1.0194
10	0.9721	0.9765	0.9811	0.9884	0.9927	0.9968	1.0033	1.0101
20	0.9654	0.9703	0.9746	0.9804	0.9851	0.9890	0.9937	1.0008
30	0.9601	0.9646	0.9687	0.9741	0.9790	0.9823	0.9873	0.9932
40		0.9596	0.9634	0.9687	0.9729	0.9768	0.9813	0.9869
50		0.9552	0.9587	0.9638	0.9680	0.9714	0.9757	0.9812
60			0.9542	0.9590	0.9633	0.9665	0.9706	0.9759
70				0.9549	0.9586	0.9619	0.9659	0.9709
80				0.9506	0.9545	0.9575	0.9615	0.9665
90					0.9503	0.9532	0.9572	0.9619
100					0.9464	0.9494	0.9530	0.9579
110					0.9424	0.9456	0.9491	0.9539
120						0.9418	0.9453	0.9501
130						0.9383	0.9418	0.9462
140							0.9383	0.9428
150							0.9350	0.9394
160								0.9362
170								0.9332

Table IV. Summary of the Pα-MS Parameters for the Tait Equation and the Sanchez–Lacombe Equation of State

Glass: Temperature Range 30–170 °C	
a_0 (cm³/g)	0.93714
a_1 (cm³/g °C)	1.3479×10^{-4}
a_2 (cm³/g °C²)	2.5444×10^{-7}
C_0 (bar)	3810
b_1 (°C⁻¹)	2.190×10^{-3}
Liquid: Temperature Range 200–260 °C	
a_0 (cm³/g)	0.89365
a_1 (cm³/g °C)	3.4864×10^{-4}
a_2 (cm³/g °C²)	5.0184×10^{-7}
C_0 (bar)	2977
b_1 (°C⁻¹)	4.074×10^{-3}
Liquid: Temperature Range 200–260 °C	
T^* (K)	827.2
P^* (bar)	4258
ρ^* (g/cm³)	1.1268
r°	3022

UCST increases or the LCST decreases with molecular weight), the Sanchez–Lacombe theory was used. Characteristic parameters, P^*, T^*, and ρ^*, reported previously for polystyrene were used;[48] however, the values employed for Pα-MS were determined here. The PVT data obtained for the liquid state are given in Table III. Severe degradation was found to occur for Pα-MS above ~260 °C, evident by an abrupt change in volume when taking the PVT data. Therefore, only data in the liquid state up to 260 °C were used. These data were fitted to the Tait equation[28–30]

$$V(P,T) = V(0,T)\left\{1 - 0.0894 \ln\left[1 + \frac{P}{C(T)}\right]\right\} \quad (24)$$

where $V(P,T)$ is the specific volume (cm³/g) at pressure P (bar) and temperatures T (°C) and the term $V(0,T)$ is the specific volume at zero pressure. The temperature dependence of $V(0,T)$ is given in polynomial form by

$$V(0,T) = a_0 + a_1 T + a_2 T^2 \quad (25)$$

while the dependence of $C(T)$ has the exponential form

$$C(T) = C_0 \exp[-b_1 T] \quad (26)$$

Parameter values obtained by fitting the equation to the data in the glassy and the liquid state are given in Table IV. The constants for Pα-MS are in good agreement with those reported by Cowie and Toporowski.[61]

A nonlinear least squares fit of the data using eq 1 and the Sanchez–Lacombe equation of state was also performed. This equation of state, while having a simple closed mathematical form, does show deviations from data at high pressures.[62,63] Thus, high-pressure data ($P > 100$ MPa) were omitted from the regression to alleviate this problem. The bottom of Table IV lists the characteristic parameters determined for the temperature range 200–260 °C and pressures of 0–100 MPa.

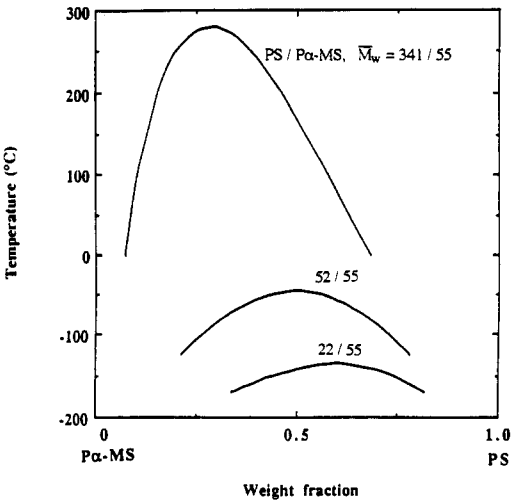

Figure 2. Predicted spinodal curves for PS/Pα-MS blends using the Sanchez–Lacombe equation of state with $\Delta P^* = 0.018$ cal/cm³. Molecular weights of polymers are indicated (e.g., 22 means 22 000).

Using the equation of state, the interaction energy was determined to lie within the range $0.011 < \Delta P^* < 0.025$ cal/cm³ using the same approach applied earlier in the Flory–Huggins analysis. Interestingly, the limits for B and ΔP^* are quite similar. This suggests that equation of state effects are not very important for this blend and that the molecular weight boundary between miscible and immiscible blends occurs because of an increase in the UCST with molecular weight. The equation of state, with ΔP^* set equal to 0.018 cal/cm³ (the average of the upper and lower limits), was used to construct the spinodal curves for the various molecular weight blends investigated, shown in Figure 2.

Upper critical solution temperature behavior has also been determined by Lin and Roe[50,57] and by Rameau et al.[59] to be the mode of phase separation. It is concluded that B and ΔP^* are essentially equal within experimental error.

PS and PMMA Blends. It is well-known that blends of PS and PMMA are immiscible at high molecular weights; however, when the molecular weight of PS and PMMA were reduced to 2950 and 2400, respectively, their blends were found to be completely miscible. Results for the various blends prepared by solution casting are given in Table II. As indicated, some blends had pure component T_g's which were too close to be resolved by DSC, and their homogeneity was solely based on visual observations.

Blends of PS(2.95) with PMMA(4.25) and with PMMA(10.55) were found to be completely miscible for all accessible temperatures at the two extremes of compositions but UCST-type behavior was seen in the mid-composition range. Cloud points (see Figure 3) were determined by optical observation and were completely reversible. The curves in Figure 3 were drawn to be consistent with T_g data that showed the blends at high and low PMMA content to be homogeneous. The cloud point curves increase with the molecular weight of PMMA as expected. Since these polymers are nearly monodisperse, the maximum in the cloud point curve should

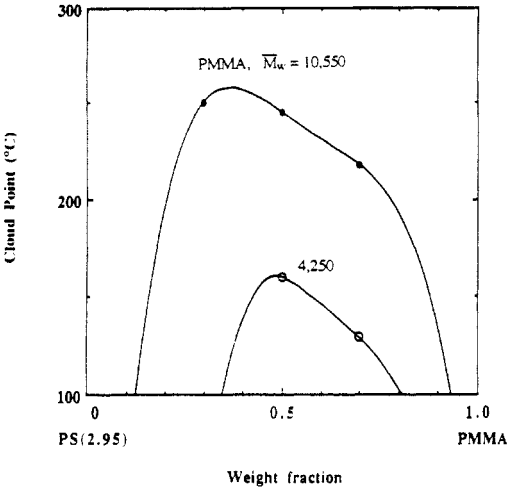

Figure 3. Visually determined cloud point temperatures of PMMA blends with PS(2.95). Molecular weights of PMMA are indicated.

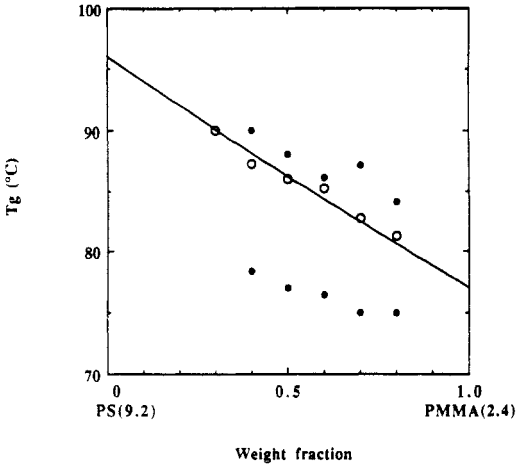

Figure 4. T_g behavior of PS(9.2)/PMMA(2.4) blends determined by DSC at 20 °C/min using the midpoint method: (●) two phase below UCST; (○) one phase after heating above 150 °C and quenching at 250 °C/min. The line drawn was calculated using the Fox equation and the measured T_g for the pure component polymers.

correspond to ϕ_c. Using eq 6 the critical weight fraction of PMMA should occur at 0.50 and 0.39 for the PMMA-(4.25) and PMMA(10.55) blends, respectively. Experimental observations appear to be consistent with these theoretical calculations. Heating above the UCST with subsequent quenching at 250 °C/min was not sufficient to trap these polymers in their homogeneous state by the DSC method. Some comments related to this issue will be made later.

Higher molecular weight PMMA (i.e., PMMA(20.3) and PMMA(60)) was also found to show UCST-type phase behavior with PS(2.95) but this occurred at temperatures much higher than 250 °C, where severe depolymerization and degradation of PMMA might influence the results. Thus, these blends were not pursued further.

Blends of PS(9.2) with PMMA(2.4) and with PMMA-(4.25) were found to be partially miscible and showed UCST-type phase behavior. The T_g behavior for blends of PS(9.2) and PMMA(2.4) is shown in Figure 4. The solid points represent phase-separated blends, while the open circles are the single T_g found after heating to 150 °C (above the UCST) and quenching in the DSC at 250 °C/min. PS(9.2) and PMMA(4.25) have very similar T_g's; however, visual methods indicate that this pair exhibits UCST-type phase separation at elevated temperatures.

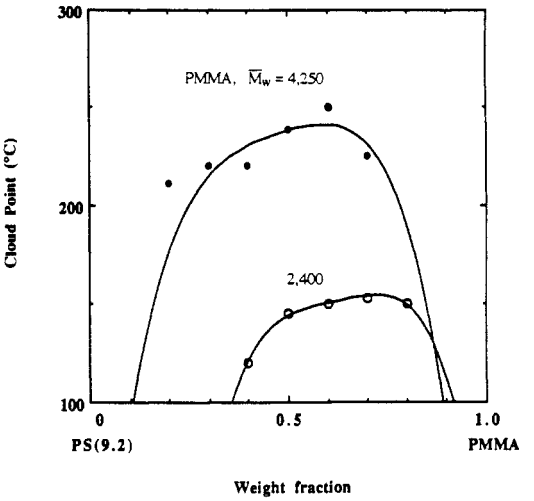

Figure 5. Visually determined cloud point temperatures of PMMA blends with PS(9.2). Molecular weights of PMMA are indicated.

Cloud points for PMMA blends with PS(9.2) shown in Figure 5 were found to be completely reversible as judged by visual observation. The curves shown were drawn to be consistent with both T_g and optical observations which indicate that blends of high and low PMMA content are homogeneous. Again, the cloud point increases with increasing PMMA molecular weight. Critical points are predicted to occur at 0.71 and 0.64 weight fraction PMMA for blends of PS(9.2) with PMMA(2.4) and with PMMA-(4.25), respectively, and the data appear to be consistent with these calculations.

It was possible to trap the PS(9.2)/PMMA(2.4) blend in its homogeneous state by quenching in the DSC, but blends of PMMA with PS(2.95), which also showed UCST behavior, always displayed two T_g's. This is believed to be a result of the diffusional mobility relative to the quenching rate. Even though the DSC was programmed to quench at 250 °C/min, the actual rate is much slower due to heat transfer limitations. Experiments indicate that the actual cooling rate is closer to 100 °C/min. Regardless of the exact rate, the cooling takes a finite amount of time. For PS(2.95)/PMMA(10.55) blends, the cloud point is roughly 150 °C above the glass transition temperature. This means at least 1.5 min is needed to cool the blend before motions are locked in, which is obviously ample time for phase separation of the low molecular weight polymers. The cloud point curves for the PS(2.95)/PMMA(4.25) and the PS(9.2)/PMMA(2.4) blends are 70 and 60 °C above T_g. While these blends must be cooled over roughly the same temperature range, it is possible to trap the PS(8.2)/PMMA(2.4) blend, but not the PS(2.95)/PMMA(4.25) blend, in a homogeneous state. Mobility is a function of many factors such as structure, temperature, viscosity, and molecular weight. Here, the main issue is the change in mobility of PS with molecular weight. As a result, the PS(2.95)/PMMA(4.25) blend is able to phase separate when cooling over this temperature interval while the PS(9.2)/PMMA(2.4) blend cannot.

Interaction energies were calculated from both the Flory–Huggins and the Sanchez–Lacombe equation of state theories using cloud point data closest to the critical composition. In principle, phase separation can begin once the binodal curve has been traversed via nucleation and growth.[64] Since the cloud point was defined as the first sign of cloudiness, it may not represent the spinodal at off-critical compositions, particularly for low molecular

Table V. Interaction Energies for PS/PMMA Blends Calculated by the Flory–Huggins (B) and Sanchez–Lacombe Equation of State (ΔP^*)[a]

polymer blend	B (cal/cm^3)	ΔP^* (cal/cm^3)	T_c (°C)	ϕ_{PMMA}
PS(2.95)/PMMA(4.25)	0.542	0.620	160	0.47
PS(2.95)/PMMA(10.55)	0.464	0.532	245	0.47
PS(9.2)/PMMA(2.4)	0.457	0.520	153	0.67
PS(9.2)/PMMA(4.25)	0.392	0.455	250	0.57

[a] From visual cloud point temperatures.

Table VI. Characteristic Parameters Used in the Sanchez–Lacombe Equation of State[a]

system	polymer	T^* (K)	P^* (MPa)	ρ^* (g/cm^3)	temp range (°C)
A	Pα-MS	827.2	425.8	1.1268	200–260
	PS	809.5	280.9	1.0922	200–260
B	PS	739.9	403.9	1.1186	150–250
	PMMA	705.2	535.4	1.2733	150–250
C	PMMA	705.2	535.4	1.2733	150–250
	Pα-MS	827.2	425.8	1.1268	200–260

[a] Values for PS and PMMA determined from PVT data reported by Kim and Paul.[48,65]

weight polymers with relatively high diffusional mobility. Because the spinodal and binodal curves converge at the critical point, any error will be minimized if the calculation is done there.

Interaction energies calculated using the Flory–Huggins theory (B) and the Sanchez–Lacombe equation of state theory (ΔP^*) are given in Table V. Characteristic parameters used in the Sanchez–Lacombe equation of state can be found in Table VI. These values were determined from PVT data, reported elsewhere,[48,65] for the temperature interval from 150 to 250 °C and a pressure range of 0–100 MPa. This temperature range was chosen because it encompasses all critical temperatures (see Table V). The cloud point temperature near the critical composition is used in the spinodal equations (5) and (17) where the interaction energy is assumed to be independent of temperature. The interaction energy extracted from the Flory–Huggins theory (B) is certain to have some temperature dependence which can be a direct reflection of either the polymer–polymer interaction or equation of state effects. The interaction parameter calculated from the Sanchez–Lacombe theory (ΔP^*) is less likely to change with temperature since equation of state effects have been stripped from it. However, temperature independence of the interaction parameter, ΔP^*, is a necessary assumption made in this analysis.[48]

The interaction energies computed by either theory (see Table V) are not the same for the various blends, and these differences could stem from effects of temperature, molecular weight, composition, or end groups. Though all of these may affect the magnitude of the interaction energy, end groups are believed to be the dominant factor. As seen in Figure 1, the PS oligomers have a butyl (Bu) end group while the PMMA oligomers have a cumyl end group, which we will later approximate as an α-methylstyrene (α-MS) unit.

Massa[66,67] in a study of blends of SMMA copolymers with PS oligomers and of PMMA with PS oligomers plotted the calculated interaction parameter versus the sum of the inverse of the molecular weights of both components. Plots of B and ΔP^* of this type are shown in Figures 6 and 7, respectively. These graphs, extrapolated to infinite molecular weights, give 0.21 ± 0.02 cal/cm^3 for B and 0.26 ± 0.02 cal/cm^3 for ΔP^* at an average temperature of 202 °C. Massa[67] obtained a B value of 0.24 ± 0.05 cal/cm^3 from his data at 195 °C by this method.

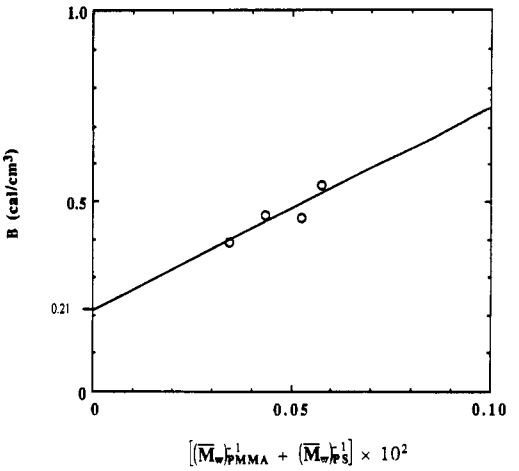

Figure 6. Molecular weight dependence of the Flory–Huggins interaction energy (B) for blends of PS and PMMA.

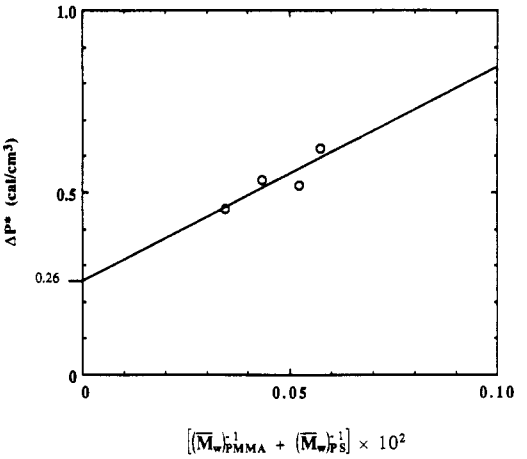

Figure 7. Molecular weight dependence of the Sanchez–Lacombe interaction energy (ΔP^*) for blends of PS and PMMA.

An alternate method based on a double extrapolation to zero volume fraction of end groups was also employed to calculate the interaction parameters. The first step was to obtain the interaction parameter at zero PMMA end group content using data for blends of PMMA with PS(9.2) and with PS(2.95). The next step was to extrapolate the results at zero PMMA end group concentration to zero PS end group content. The values from this double extrapolation, 0.27 cal/cm^3 for B and 0.33 cal/cm^3 for ΔP^*, should be free of contributions from both PS and PMMA ends groups.

Finally, the binary interaction model, eq 22, was used to deal with the issue of end groups as suggested previously by Fleischer and Koberstein.[68] Each oligomer is composed of two types of groups, the monomer repeat unit and an end group (Bu for PS and α-MS for PMMA), whose volume fractions vary as molecular weight is changed. Thus, there are six unknown B_{ij} values in eq 22, whereas we have only four equations from experimental observations. Therefore, two B_{ij} must be known from other sources to solve the four equations simultaneously. For these, we use the S/α-MS interaction (B = 0.018, ΔP^* = 0.018) established in the previous section and the S/Bu interaction (B = 4.0, ΔP^* = 4.5) whose determination has been described elsewhere.[69] Solving the four equations simultaneously yields B = 0.26 cal/cm^3 and ΔP^* = 0.32 cal/cm^3 for the S/MMA interaction energy. The other interaction parameters deduced by this analysis are B = 9.6 and ΔP^* = 11.4 for MMA/Bu; B = 82 and ΔP^* = 108 for α-MS/Bu; and B = −2.1 and ΔP^* = −1.9 cal/cm^3 for MMA/α-MS.

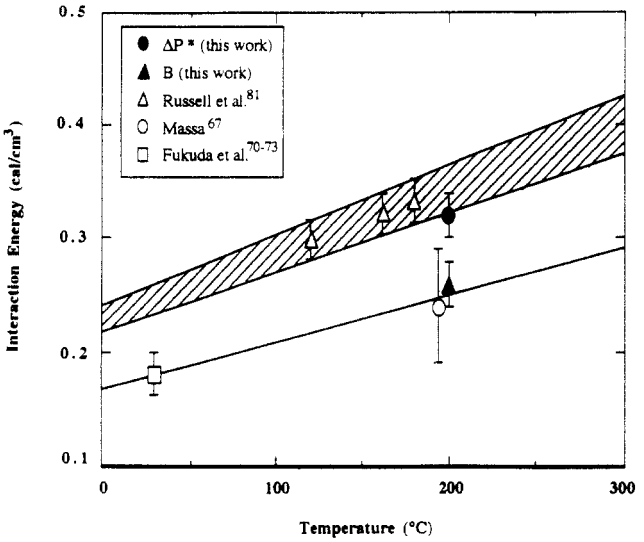

Figure 8. Temperature dependence of the interaction energy for PS/PMMA blends found by various authors. Estimated errors are indicated; shaded region encompasses error reported by Russell.[81]

Table VII. Interaction Energies for PS/PMMA Blends Determined by the Various Extrapolation Methods

interaction energy (cal/cm³)	extrap from Figures 6 and 7	double extrap	binary interaction model
$B_{S/MMA}$	0.21 ± 0.02	0.27	0.26 ± 0.02
$\Delta P^*_{S/MMA}$	0.26 ± 0.02	0.33	0.32 ± 0.02

Values of the S/MMA interaction determined by these three methods are relatively close and are summarized in Table VII. We believe the binary interaction model provides the best estimate since the method has some theoretical foundation and employs additional information to reduce the degrees of freedom in parameter estimation or extrapolation. The S/MMA interaction has been studied by numerous techniques,[66,67,69-81] and the values reported for B range from 0.04 to 0.34 cal/cm³. Some reported values are given as χ and must be converted to the energy density term B. This is straightforward if the reference volume is stated, but this conversion may be somewhat ambiguous, as pointed out by Nishimoto et al.[82] The reported values were determined at temperatures from 30 to 200 °C but in some instances the temperature was not well-defined. Temperature undoubtedly affects the interaction parameter, and this is one cause for some of the discrepancy in the reported values.

The most comprehensive study of the effect of temperature to this date is the work of Russell et al.[81] Their results are based on small-angle neutron scattering (SANS) of a symmetric, diblock copolymer, P(S-*b*-PMMA), where the PS block was deuterated. Reported values from selected authors are shown in Figure 8, where the shaded region indicates the experimental error reported by Russell et al. If we group the values into two sets, it is apparent that the temperature dependence given by Russell et al. seems to apply to both sets; however, their absolute magnitudes differ by approximately 20%. Deuteration has been shown to influence the temperature at which blends phase separate by altering the interaction energy.[50,64,83] This effect is likely to be greatest on a relative basis for weakly interacting systems. Since the S/MMA interaction energy is quite small, it is likely that some finite contribution from deuteration is reflected in the values reported by Russell et al. End groups may affect the scattering profile in various ways including the direct thermodynamic one described above, affecting the computed S/MMA interaction energy. Block copolymers of varying block lengths need to be studied to establish the magnitude of this possibility.

Our value of ΔP^* for S/MMA is 22% greater than the B calculated from the same experimental results. Interestingly, this ΔP^* is about the same as the B from Russell et al. Some of the difference between B and ΔP^* stems from compressibility effects, and eq 20 provides a connection between the two.

By using eq 20, ΔP^* is predicted to be approximately 13% greater than B due to equation of state effects. From our values the compressibility of the system accounts for more than half of the 22% difference between B and ΔP^* found experimentally. The rest of the difference (9%) is contained within the experimental error. A potential source of error in this analysis lies in the assumption that the characteristic parameters for the polymers can be used for the oligomers. Both the end groups and molecular weight per se may affect the PVT behavior and, thus, the characteristic parameters. Ougizawa et al.[84] have shown that the characteristic parameters of polystyrene for the Flory equation of state[44,85] and the cell model equation of state[63] are dependent upon the molecular weight. Over a range of more than 3 orders of magnitude in polystyrene molecular weight, the characteristic volume increased by 2%, the characteristic temperature decreased by 8%, and the characteristic pressure remained constant (within experimental error) with decreasing molecular weight. The lowest molecular weight used in the study by Ougizawa et al. was $\bar{M}_w$ = 910. The PVT behavior of PS(341) and PS(0.680) was determined, and the same trends in characteristic parameters with molecular weight were found using the Sanchez–Lacombe equation of state. The percent change in these parameters was similar to those found by Ougizawa et al.[84] Due to a limited supply of the low molecular weight polymers and the large amount of sample needed for the PVT measurements, the slight dependencies of the characteristic parameters on molecular weight were ignored. A more significant issue is the effect of end groups on the interaction energy which in turn alters the phase diagram. By correction for this as described above, interaction energies representative of repeat unit pairs can be determined.

The Sanchez–Lacombe theory can be used to compute the temperature-dependent Flory–Huggins interaction parameter and its enthalpic (eq 15) and entropic (eq 16) parts as shown in Figure 9 for a 60 wt % PMMA blend of PS(9.2) and PMMA(4.25). A key assumption is that the "bare" interaction parameter is temperature independent. Therefore, any temperature dependence of $B(T)$ is assumed to be due to equation of state effects. In Figure 9 the enthalpic contribution, B^h, decreases with temperature while the entropic contribution, $-TB^s$, increases. These opposing effects partially offset each other and the temperature-dependent interaction, $B(T) = B^h - TB^s$, increases only slightly with temperature and is given by

$$B(T) = 0.542 + (1.00 \times 10^{-4})T \qquad (27)$$

where T is in degrees Kelvin.

Calorimetric studies by Brannock et al.[86] have resulted in a ΔP^* value of 0.32 cal/cm³ for the S/MMA interaction energy. This is in agreement with the value found here of 0.32 cal/cm³.

Kim and Paul[65] recently described a thermodynamic analysis of blends of tetramethyl-Bisphenol-A polycarbonate with SMMA copolymers. A value of ΔP^* for the S/MMA interaction of 0.15 cal/cm³ was reported, but

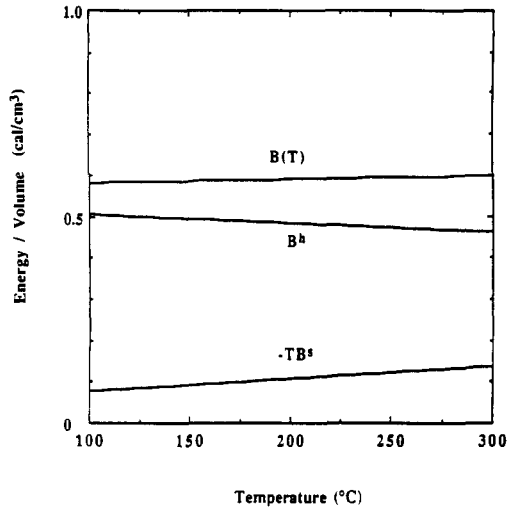

Figure 9. Temperature dependence of the extended Flory–Huggins interaction energy and its enthalpic and entropic components for a PS(9.2)/PMMA(4.25) blend containing 60 wt % PMMA.

reexamination of these results has revealed a calculation error and the revised value is $\Delta P^* = 0.25$ cal/cm^3.[69] The latter is more consistent with the results reported here.

PMMA and Pα-MS Blends. Blends of PMMA and Pα-MS have not been as intensely studied as the two previous systems. Interactions have generally been determined from blends of copolymers. This information is sought here by blending low molecular weight versions of the two homopolymers; however, corrections for end group effects must be made to extract the interaction energies as shown in the following.

The various blends investigated are summarized in Table II. Blends of PMMA(1.21) with Pα-MS of molecular weights up to 19 500 were found to be miscible and showed no phase separation on heating or cooling. All blends were clear with a T_g well approximated by the Fox equation.

Blends of PMMA(2.4) and Pα-MS(6.7) were found to be one phase at low temperatures and to phase separate at elevated temperatures. Blends were homogeneous as prepared, but after heating above 250 °C and rapid quenching in the DSC, some showed two distinct T_g's. Thus, it was possible to trap some of the blends in a heterogeneous state.

Blends of PMMA(4.25) with Pα-MS(3.5) and with Pα-MS(6.7) were also found to be one phase at low temperatures and showed LCST-type phase behavior. The glass transition temperatures for blends of PMMA(4.25) with Pα-MS(6.7) are shown in Figure 10. It was possible to trap all blends in a heterogeneous state by quenching in the DSC. Quenching was more successful here because of the proximity of the LCST to the blend T_g and because of the higher molecular weights involved which reduce the mobility of the chains.

The cloud points in Figure 11, determined by visual observation, shift to lower temperatures as molecular weight increases as expected. Curves are drawn to reflect blends which are miscible at high and low PMMA content as indicated by their T_g behavior. Critical points are in agreement with those calculated by eq 6. All phase boundaries in Figure 11 were found to be reversible by annealing, but the time to reach equilibrium increased as the molecular weight increased. Blends of PMMA(2.4)/Pα-MS(6.7) took 10 min to establish equilibrium, PMMA(4.25)/Pα-MS(3.5) blends took 20 min to reach equilibrium, and PMMA(4.25)/Pα-MS(6.7) blends took 2 h before

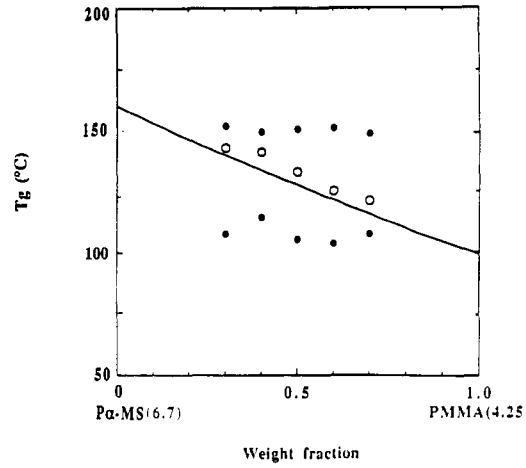

Figure 10. T_g behavior of PMMA(4.25)/Pα-MS(6.7) blends determined by DSC at 20 °C/min using the midpoint method: (○) one phase below LCST; (●) two phase after heating above 200 °C and quenching at 250 °C/min. The line drawn was calculated using the Fox equation and the measured T_g for the pure component polymers.

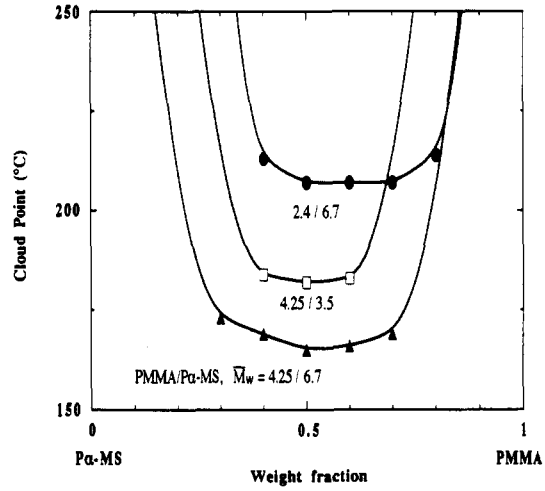

Figure 11. Visually determined cloud point temperatures of PMMA/Pα-MS blends. Molecular weights of polymers are indicated.

phase-separated blends became homogeneous (transparent). This is primarily the result of reduced mobility (higher viscosity) as the phase boundary approaches the glass transition temperature caused by the increase in molecular weight. Of course, the increased molecular weight per se also reduces mobility.

A higher molecular weight poly(methyl methacrylate), PMMA(10.55), was blended with Pα-MS(3.5) and found to be immiscible. The blends exhibited one T_g on the first heating in the DSC and two T_g's in subsequent scans. This is indicative of LCST-type behavior, but after 24 h of annealing the blends below their suspected phase separation temperature (~150 °C), blend homogeneity was not found so the blend was considered immiscible. Undoubtedly, the blends are trapped in a nonequilibrium state when cast at ~50 °C. Likewise, trapping of PC/PMMA blends in nonequilibrium states has also been reported.[87]

The binary interaction model, eq 22, was used to obtain interaction energies between the MMA and α-MS repeat units by correcting for the effects of the oligomer end groups (see Figure 1 and Table I). The end group on the PMMA oligomer is approximated as an α-MS unit, which

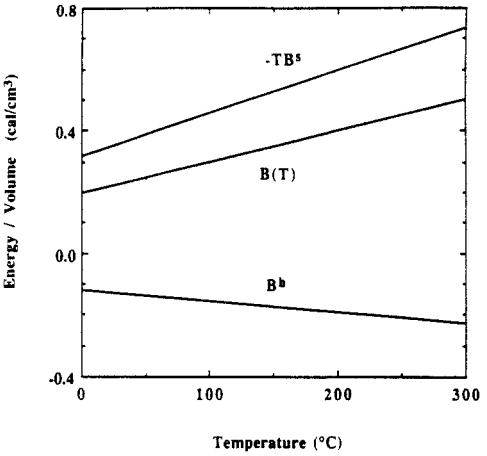

Figure 12. Temperature dependence of the extended Flory–Huggins interaction energy and its enthalpic and entropic components for a PMMA(4.25)/Pα-MS(6.7) blend containing 50 wt % PMMA.

allows eq 22 to be simplified by setting 2 = 3, i.e.

$$B = B_{12}\phi_1'^2 + B_{24}\phi_4''^2 + (B_{14} - B_{12} - B_{24})\phi_1'\phi_4'' \quad (28)$$

where 1 = MMA, 2 = 3 = α-MS, and 4 = Bu. The assumption made here is that the intermolecular and intramolecular interactions are equal, which Cowie et al. have suggested may not always be the case.[88] The equation for ΔP^* can be written by analogy.

The net interaction parameter ΔP^* for each blend was calculated from the experimental cloud points (Figure 11) using eqs 17–19. The ΔP^* equivalent of eq 28 was then used to extract the individual interaction energies. Characteristic parameters used are given in Table VI. The temperature range of 150–250 °C for PMMA includes all critical temperatures (see Figure 11). The same temperature range for Pα-MS cannot be used due to the high T_g of Pα-MS; use of the more limited range for Pα-MS seems to be a reasonable alternative.[89] Three equations result with three unknowns each; however, direct solution of these simultaneous equations leads to unrealistic magnitudes of the interaction parameters. This is due to the small variation in ΔP^* since the end group concentrations are relatively low and do not vary much. Therefore another approach was used. The assumption is made that the interaction between α-MS and Bu is equal to that between S and Bu which has been determined to be $B = 4.0$ cal/cm^3 and $\Delta P^* = 4.5$ cal/cm^3.[69] Using these values along with the net interaction energy calculated by the Sanchez–Lacombe equation of state for the two highest molecular weight blends (lowest end group contribution), we get $B = 0.26$ cal/cm^3 and $\Delta P^* = -0.084$ cal/cm^3 for the MMA/α-MS pair. The net Flory–Huggins interaction energy, B, for the blend used here is taken from that predicted by the equation of state at the spinodal condition, B_{sc} (see eq 20).

Using the extended Flory–Huggins theory, the interaction parameter, B, can be represented by enthalpic (B^h) and entropic ($-TB^s$) parts (see eqs 15 and 16). The temperature dependence of each term due to equation of state effects is shown in Figure 12 for a 50 wt % blend of PMMA(4.25) and Pα-MS(6.7). The term B^h, which is related to the heat of mixing, is negative and decreases slightly with increasing temperature. The fact that the heat of mixing and ΔP^* are predicted to be negative suggests there is a weakly favorable interaction for this pair.

The term $-TB^s$ is positive and increases quite dramatically as the temperature is raised. The large entropic contribution causes the net interaction parameter $B(T)$ to be positive and to increase with increasing temperature. The temperature dependence of B in Figure 12 is given by

$$B(T) = -0.0833 + (1.034 \times 10^{-3})T \quad (29)$$

for the PMMA(4.25)/Pα-MS(6.7) blend, where T is the temperature in degrees Kelvin.

The interaction parameter, B, reported by Cowie et al. for MMA/α-MS is 0.104 cal/cm^3 at 25 °C.[90] This is considerably lower than the value found here of 0.26 cal/cm^3. However, by considering the temperature dependence of the interaction parameter, this difference can be resolved. Using the value 0.26 cal/cm^3 at 185 °C for the MMA/α-MS pair, using the same temperature dependence found for the PMMA(4.25)/Pα-MS(6.7) blend, and extrapolating to 25 °C gives a value of 0.096 cal/cm^3, which, within experimental error, agrees with the value from Cowie et al.

Another investigation in our laboratory on blends of PMMA and α-MSAN copolymers has yielded a value of $\Delta P^* = 0.05$ cal/cm^3 for the MMA/α-MS interaction energy.[91] The possibility of end group effects on this value is also under investigation at this time. The differences between these two very small values of ΔP^* may simply be within the experimental uncertainty of the methods employed. In any case it is clear that the α-methyl addition to styrene significantly reduces the interaction energy with PMMA.

It is instructive to investigate the cause for phase instability that drives PMMA/Pα-MS blends to phase separate by an LCST-type phase boundary. Inspection of eq 17 reveals that only the following two terms can drive $d\mu/d\phi_1$ to be negative or cause phase separation: $-\tilde{\rho}\Delta P^*$ or $-(kT/2v^*)\tilde{\rho}\tilde{\Psi}^2\tilde{T}P^*\beta$. The first may be positive or negative depending on the sign of ΔP^*. However, if ΔP^* itself is not temperature dependent, as frequently assumed in the absence of strong specific interactions,[48,65,92] then this term will always be only a weak function of temperature through $\tilde{\rho}$. Therefore, we focus on the second term since each individual factor is positive and, thus, it tends to destabilize the blend at all temperatures. The magnitude of this term determines what effect it has on phase behavior. The factor $(kT/2v^*)\tilde{\rho}\tilde{T}P^*\beta$ increases slightly with temperature, but Ψ^2 (see eq 18) may be significantly more temperature dependent. Change in Ψ can be the dominant factor affecting the stability of the blend (making $d\mu/d\phi_1$ negative). The first term in the numerator of eq 18 is proportional to $T^*_1 - T^*_2$, or ΔT^*, and can become the most important one depending on the value of ΔT^*. The ΔP^* term will be less than the ΔT^* term by at least an order of magnitude for any reasonable value of ΔP^* even when the T^*'s differ by as little as 20 °C. The only exception to this is for extremely asymmetric blends ($v^*_1 \ll v^*_2$) or at the extremes of composition (approaching the pure components). The $(1/r^\circ_i)$ term is generally negligible even for these low molecular weight polymers and the final term is always negligible except at extremely high pressures. Therefore, the phase separation is driven by the large difference in the T^*_i values which is related to the affinity the pure polymers have for their own kind.[19]

Because of the imperfect nature of the equation of state, the characteristic parameters depend on the temperature range over which the PVT data are fitted. To a certain extent, the interaction energies and predicted phase behavior deduced from the theory depend on this choice. For example, refitting the PMMA data over the range

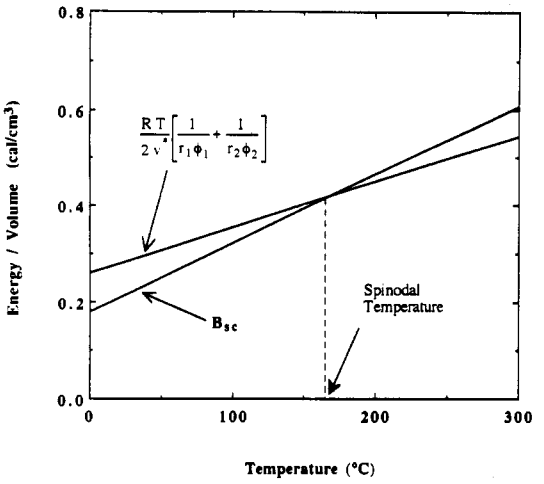

Figure 13. Effect of temperature on B_{sc} and the combinatorial entropy term at the spinodal condition for a PMMA(4.25)/Pα-MS(6.7) blend containing 50 wt % PMMA. The intersection of the two lines gives the spinodal temperature.

200–250 °C leads to $T^* = 732.1$ K versus the value of 705.2 K, obtained for the range 150–250 °C, used above. This results in some reduction in the contribution from the equation of state effect; i.e., ΔT^* is reduced from 122 to 95.1 °C. However, as explained earlier, we feel that the ranges and parameters given in Table VI are a more logical choice. Clearly, there is a need to find a way to minimize this troublesome feature of the analysis, and approaches to accomplish this are being explored.

Figure 13 compares the combinatorial entropy and B_{sc} (calculated from the Sanchez–Lacombe theory) terms of the Flory–Huggins theory for a 50 wt % blend of PMMA-(4.25)/Pα-MS(6.7). For this low molecular weight blend, the combinatorial entropy contribution increases with temperature but is overcome by the more rapidly increasing B_{sc} with temperature (caused by equation of state effects). The intersection of these two lines is the spinodal point where phase separation occurs as required by eq 3.

Cowie et al. recently reported on blends of PMMA and Pα-MS where it was observed that the method of blend preparation played an important role in determining its homogeneity.[93] These blends were composed of high molecular weight polymers, and an apparent cloud point curve (LCST type) was observed above the T_g of the blend. Cowie et al. were unable to establish reversibility of the cloud points. They concluded that phase rehomogenization was either kinetically unfavorable at these low annealing temperatures or that the one-phase blends do not reflect a thermodynamic equilibrium state and are, therefore, an artifact of the method of preparation. In light of the study presented here, we believe the latter conclusion is the correct one. Calculation of the spinodal curve using the Sanchez–Lacombe equation of state shows that the LCST for the blend studied by Cowie et al.[93] should occur at about −35 °C.

Summary

These studies demonstrate that the critical molecular weight aproach can be a useful way to gain information about positive interaction energies. However, corrections for end group effects were found to be necessary. Values of the interaction energies determined here are summarized in Table VIII. Interaction energies calculated from the Sanchez–Lacombe theory, ΔP^*, and the Flory–Huggins theory, B, are essentially the same for the PS/Pα-MS pair when the upper and lower estimates are averaged. The B values that describe the interaction of PMMA with PS and with Pα-MS are essentially identical; however, the corresponding ΔP^* values are considerably different for the two systems. Differences between B and ΔP^* arise from equation of state effects which are important in both blends but in different ways. The B value for the PS/PMMA system is less than ΔP^* because there is only a small difference in the characteristic temperatures ($\Delta T^* = 35$ K) for these two components. The B value for the PMMA/Pα-MS system is larger than ΔP^* because of the large difference in the characteristic temperatures ($\Delta T^* = 122$ K) of these components. The observations of UCST-type phase boundaries in the PS/PMMA system and the LCST-type boundaries in the Pα-MS/PMMA system can be attributed to the fact that Pα-MS has a much higher value of T^* than does PS (whose value is only slightly greater than that for PMMA).

Table VIII. Summary of Interaction Energies from This Work[a]

	MMA		S	
	B	ΔP^*	B	ΔP^*
S	0.26[b]	0.32		
α-MS	0.26[c]	−0.084	0.018[d]	0.018[d]
MMA			0.26[b]	0.32

[a] All values given in cal/cm³. [b] Calculated at 202 °C, the average critical temperature. [c] B_{sc} calculated from the Sanchez–Lacombe equation of state at 185 °C. [d] Average value taken from upper and lower estimates for this pair at 50 °C.

Acknowledgment. The authors wish to thank Dennis J. Massa for the use of his data and for his helpful comments. This research was supported by the National Science Foundation, Grant No. DMR-89-00704 administered by the Division of Material Research—Polymers Program. T.A.C. acknowledges the Plastics Institute of America for fellowship support.

References and Notes

(1) Paul, D. R.; Newman, S., Eds. *Polymer Blends*; Academic Press: New York, 1978.
(2) Walsh, D. J.; Higgins, J. S.; Maconnachie, A., Eds. *Polymer Blends and Mixtures*; Martinus Nijhoff Publishers: Dordrecht, The Netherlands, 1985.
(3) Manson, J. A.; Sperling, L. H. *Polymer Blends and Composites*; Plenum Press: New York, 1976.
(4) Klempner, D.; Frisch, K. C., Eds. *Polymer Alloys*; Plenum Press: New York, 1977, 1980, 1983; Vols. I, II, III.
(5) Martuscelli, E.; Palumbo, R.; Kryszewski, M., Eds. *Polymer Blends: Processing, Morphology and Properties*; Plenum Press: New York, 1980.
(6) Han, C. D., Ed. *Polymer Blends and Composites in Multiphase Systems*; Adv. Chem. Ser. No. 206, American Chemical Society: Washington, DC, 1984.
(7) Flory, P. J. *Principles of Polymer Chemistry*; Cornell University Press: Ithaca, NY, 1953.
(8) Hoffman, J. D.; Weeks, J. J. *J. Res. Natl. Bur. Stand.* **1962**, *66*, 13.
(9) Weeks, N. E.; Karasz, F. E.; MacKnight, W. J. *J. Appl. Phys.* **1977**, *48*, 4068.
(10) Cruz, C. A.; Barlow, J. W.; Paul, D. R. *Macromolecules* **1979**, *12*, 726.
(11) Kruse, A. C.; Kirste, R. G.; Haas, J.; Schmitt, B. J.; Stein, D. J. *Makromol. Chem.* **1976**, *117*, 1145.
(12) Harris, J. E.; Paul, D. R.; Barlow, J. W. *Polym. Eng. Sci.* **1983**, *23*, 676.
(13) Kwei, T. K.; Nishi, R.; Rorets, R. F. *Macromolecules* **1974**, *7*, 667.
(14) Kambour, R. P.; Gundlach, P. E.; Wang, I. C. W.; White, D. M.; Yeager, G. W. *Polym. Commun.* **1988**, *29*, 170.
(15) Patterson, D. *Macromolcules* **1969**, *2*, 672.
(16) Sanchez, I. C. In *Encyclopedia of Physical Science and Technology*; Meyers, R. A., Ed.; Academic Press: New York, 1987; Vol. 11.
(17) Sanchez, I. C.; Lacombe, R. H. *J. Phys. Chem.* **1976**, *80*, 2352.

(18) Sanchez, I. C.; Lacombe, R. H. *J. Polym. Sci., Polym. Lett. Ed.* **1977**, *15*, 71.
(19) Sanchez, I. C.; Lacombe, R. H. *Macromolecules* **1978**, *11*, 1145.
(20) Kambour, R. P.; Bendler, J. T.; Bopp, R. C. *Macromolecules* **1983**, *16*, 753.
(21) ten Brinke, G.; Karasz, F. E.; MacKnight, W. J. *Macromolecules* **1983**, *16*, 1827.
(22) Paul, D. R.; Barlow, J. W. *Polymer* **1984**, *25*, 487.
(23) *PL—Polymer Standards Handbook*; Polymer Laboratories: Church Stretton, U.K.
(24) Lane, J., private communication, Polymer Laboratories Inc., PLI Fax Ref. No. 1940, Jan 23, 1992.
(25) Ziegler, K.; Dislich, H. *Ber.* **1957**, *90*, 1107.
(26) Szwarc, M. *Carbanions, Living Polymers, and Electron Transfer Processes*; Interscience Publishers: New York, 1968; Chapter 3.
(27) Zoller, P.; Bolli, P.; Pahud, V.; Ackermann, H. *Rev. Sci. Instrum.* **1976**, *47*, 948.
(28) Quach, A.; Simha, R. J. *Appl. Phys.* **1971**, *42*, 4592.
(29) Boyer, R. F. *Macromolecules* **1982**, *15*, 774.
(30) Zoller, P. *J. Polym. Sci., Polym. Phys. Ed.* **1978**, *16*, 1261.
(31) Sanchez, I. C. In *Polymer Blends*; Paul, D. R., Newman, S., Eds.; Academic Press: New York, 1978; Vol. 1.
(32) Sanchez, I. C. *Annu. Rev. Mater. Sci.* **1983**, *13*, 387.
(33) Sanchez, I. C.; Balazs, A. C. *Macromolecules* **1989**, *22*, 2325.
(34) Sanchez, I. C. *Polymer* **1989**, *30*, 471.
(35) Rodgers, P. A. Ph.D. Dissertation, The University of Texas at Austin, 1990.
(36) Flory, P. J. *J. Chem. Phys.* **1942**, *10*, 51.
(37) Huggins, M. L. *J. Chem. Phys.* **1941**, *9*, 440.
(38) Paul, D. R.; Barlow, J. W.; Keskkula, H. In *Encyclopedia of Polymer Science and Engineering*, 2nd ed.; Mark, H. F., Bikales, N. M., Overberger, C. G., Menges, Eds.; John Wiley: New York, 1988; Vol. 12, p 399.
(39) Koningsveld, R.; Chermin, H. A. G. *Proc. R. Soc. London, A* **1970**, *319*, 331.
(40) Koningsveld, R. *Br. Polym. J.* **1975**, *7*, 435.
(41) Koningsveld, R.; Kleintjens, L. A. *J. Polym. Sci., Polym. Symp.* **1977**, *No. 61*, 221.
(42) Koningsveld, R.; Schoffeleers, H. M. *Pure Appl. Chem.* **1974**, *39*, 1.
(43) Flory, P. J. *J. Am. Chem. Soc.* **1965**, *87*, 1831.
(44) Eichinger, B. E.; Flory, P. J. *Trans. Faraday Soc.* **1968**, *64*, 2035.
(45) Simha, R. *Macromolecules* **1977**, *10*, 1025.
(46) Patterson, D.; Robard, A. *Macromolecules* **1978**, *11*, 690.
(47) Panayiotou, C. G. *Macromolecules* **1987**, *20*, 861.
(48) Kim, C. K.; Paul, D. R. *Polymer* **1992**, *33*, 1630.
(49) Kim, J. H.; Barlow, J. W.; Paul, D. R. *J. Polym. Sci., Polym. Phys. Ed.* **1989**, *27*, 223.
(50) Lin, J.; Roe, R. *Macromolecules* **1987**, *20*, 2168.
(51) Robeson, L. M.; Matzner, M.; Fetters, L. J.; McGrath, J. E. *Recent Advances in Polymer Blends, Grafts, and Blocks*; Sperling, L. H., Ed.; Plenum Press: New York, 1974; p 281.
(52) Dunn, D. J.; Krause, S. *J. Polym. Sci., Polym. Lett. Ed.* **1974**, *12*, 591.
(53) Gaur, U.; Wunderlich, B. *Macromolecules* **1980**, *13*, 1618.
(54) Saeki, S.; Cowie, J. M. G.; McEwen, I. J. *Polymer* **1983**, *24*, 60.
(55) Lau, S.; Pathak, J.; Wunderlich, B. *Macromolecules* **1982**, *15*, 1278.
(56) Cowie, J. M. G.; McEwen, I. J. *Polymer* **1985**, *26*, 1662.
(57) Lin, J.; Roe, R. *Polymer* **1988**, *29*, 1227.
(58) Widmaier, J. M.; Mignard, G. *Eur. Polym. J.* **1987**, *23*, 989.
(59) Rameau, A.; Gallot, Y.; Marie, P.; Farnoux, B. *Polymer* **1989**, *30*, 386.
(60) Yang, H.; Ricci, S.; Collins, M. *Macromolecules* **1991**, *24*, 5218.
(61) Cowie, J. M. G.; Toporowski, P. M. *J. Macromol. Sci., Phys.* **1969**, *B3*, 81.
(62) Zoller, P. *J. Polym. Sci., Part B: Polym. Phys.* **1980**, *20*, 157.
(63) Dee, G. T.; Walsh, D. J. *Macromolecules* **1988**, *21*, 811.
(64) Higgins, J. S. In *Polymer Blends and Mixtures*; Walsh, D. J., Higgins, J. S., Maconnachie, A. E., Eds.; Martinus Nijhoff Publishers: Dordrecht, The Netherlands, 1985.
(65) Kim, C. K.; Paul, D. R. *Polymer* **1992**, *33*, 2089.
(66) Massa, D. J. *Adv. Chem. Ser.* **1979**, *176*, 433.
(67) Massa, D. J. Eastman Kodak Co., private communication, February 1992.
(68) Fleischer, C.; Koberstein, J. *Polym. Prepr. (Am. Chem. Soc., Div. Polym. Chem.)* **1990**, *31*, 541.
(69) Callaghan, T. A. Ph.D. Dissertation, The University of Texas at Austin, 1992.
(70) Fukuda, T.; Inagaki, H. *Pure Appl. Chem.* **1983**, *55*, 1541.
(71) Fukuda, T.; Nagata, M.; Inagaki, H. *Macromolecules* **1984**, *17*, 548.
(72) Fukuda, T.; Nagata, M.; Inagaki, H. *Macromolecules* **1986**, *19*, 1411.
(73) Fukuda, T.; Nagata, M.; Inagaki, H. *Macromolecules* **1987**, *20*, 654.
(74) Nagata, M.; Fukuda, T.; Inagaki, H. *Macromolecules* **1987**, *20*, 2173.
(75) Benoit, H.; Wu, W.; Benmouna, M.; Mozer, B.; Bauer, B.; Lapp, A. *Macromolecules* **1985**, *18*, 986.
(76) Russell, T. P.; Coulon, G.; Deline, V. R.; Miller, D. C. *Macromolecules* **1989**, *22*, 4600.
(77) Brannock, G. R.; Barlow, J. W.; Paul, D. R. *J. Polym. Sci., Part B: Polym. Phys.* **1991**, *29*, 413.
(78) Dondos, A.; Benoit, H. *Makromol. Chem.* **1968**, *118*, 165.
(79) Tsitsilianis, C.; Staikos, G. *Macromolecules* **1992**, *25*, 910.
(80) Cerny, L. C.; Newman, E. H.; Stasiw, D. M.; Visalli, W. *J. Macromol. Sci., Phys.* **1973**, *B7*, 19.
(81) Russell, T. P.; Hjelm, R. P.; Seeger, P. A. *Macromolecules* **1990**, *23*, 890.
(82) Nishimoto, M.; Keskkula, H.; Paul, D. R. *Polymer* **1991**, *32*, 1274.
(83) Atkin, A. L.; Kleintjens, L. A.; Koningsveld, R.; Fetters, L. J. *Polym. Bull.* **1982**, *9*, 347.
(84) Ougizawa, T.; Dee, G. T.; Walsh, D. J. *Polymer* **1989**, *30*, 1675.
(85) Flory, P. J.; Orwoll, R. A.; Vrij, A. *J. Am. Chem. Soc.* **1964**, *86*, 3567.
(86) Brannock, G. R.; Barlow, J. W.; Paul, D. R. *J. Polym. Sci., Part B: Polym. Phys.* **1991**, *29*, 413.
(87) Nishimoto, M.; Keskkula, H.; Paul, D. R. *Polymer* **1991**, *32*, 272.
(88) Cowie, J. M. G.; Elexpuru, E. M.; McEwen, I. J., to be published.
(89) Sanchez, I. C., private communication, May 1991.
(90) Cowie, J. M. G.; Elexpuru, E. M.; McEwen, I. *J. Polym. Sci., Part B: Polym. Phys.* **1991**, *29*, 407.
(91) Gan, P. P. The University of Texas at Austin, unpublished results.
(92) Brannock, G. R. Ph.D. Dissertation, The University of Texas at Austin, 1990.
(93) Cowie, J. M. G.; Miachon, S. *Macromolecules* **1992**, *25*, 3295.